Journal of Materials Chemistry A

Accepted Manuscript

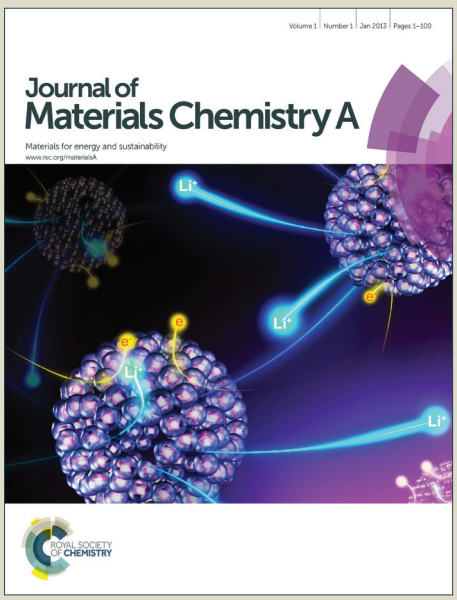

This is an *Accepted Manuscript*, which has been through the Royal Society of Chemistry peer review process and has been accepted for publication.

Accepted Manuscripts are published online shortly after acceptance, before technical editing, formatting and proof reading. Using this free service, authors can make their results available to the community, in citable form, before we publish the edited article. We will replace this *Accepted Manuscript* with the edited and formatted *Advance Article* as soon as it is available.

You can find more information about *Accepted Manuscripts* in the Information for Authors.

Please note that technical editing may introduce minor changes to the text and/or graphics, which may alter content. The journal's standard Terms & Conditions and the Ethical guidelines still apply. In no event shall the Royal Society of Chemistry be held responsible for any errors or omissions in this *Accepted Manuscript* or any consequences arising from the use of any information it contains.

ROYAL SOCIETY OF CHEMISTRY

www.rsc.org/materialsA

A dispersion-corrected DFT study on adsorption of battery active materials anthraquinone and its derivatives on monolayer graphene and *h*-BN

Yang-Xin Yu[1]*

ABSTRACT

9,10-anthraquinone (AQ) and its derivatives, i.e., benzofuro[5,6-b]furan-4,8-dione (BFFD), benzo[1,2-b: 4,5-b']dithipphene-4,8-dione (BDTD) and pyrido[3,4-g]isoquinoline-5,10-dione (PID), are environmentally friendly and cheap electrode materials. However, their significant solubility in the electrolyte solutions limits the cycle performance of lithium-ion batteries. In this work a comparative investigation of these four organic molecules adsorbed on monolayer graphene and hexagonal boron nitride (*h*-BN) is carried out using a van der Waals dispersion (vdW)-corrected density-functional theory (DFT). The calculated results indicate that the vdW dispersion contributes more than 80% of the total attractive interaction for all the complexes studied. The binding energies range from 1.06 to 1.31eV, showing a strong physisorption. The calculated binding energies of the four organic molecules are in the order: BFFD < BDTD < AQ <PID on monolayer graphene and BFFD < BDTD < PID <AQ on monolayer BN. The physisorption causes a work function shift relative to the isolated graphene or BN nanosheet in the order: AQ < BDTD < BFFD < PID on both graphene and BN nanosheets. This sequence is dominated by the ionization potentials of the four organic molecules. The strong physisorption suggests that the solubility of the four organic compounds in the electrolyte solutions can be

[1] Laboratory of Chemical Engineering Thermodynamics, Department of Chemical Engineering, Tsinghua University, Beijing 100084, P. R. China. E-mail: yangxyu@mail.tsinghua.edu.cn

Electronic supplementary information (ESI) available: Additional figures. See DOI: 10.1039/

Journal of Materials Chemistry A Accepted Manuscript

reduced by binding them to a graphene or BN nanosheet, making the organic compound-graphene or organic compound-BN composite a promising electrode material of lithium-ion batteries.

1. INTRODUCTION

Lithium-ion batteries are widely used energy storage devices for portable electronics and electric vehicles due to their high-energy density and long life.[1,2] Recently, they have been reported to be applied to grid storage.[3] Most consumer batteries still use the original lithium transition-metal oxide cathodes and graphite anodes until now.[4] However, toxicity, safety and resource availability are known problems with lithium transition metal oxides.[1] Alternatively, organic compounds offer new possibilities for high energy density, environmentally friendly and cheap electrode materials.[5-8] Some of these organic molecules can be generated from biomass,[6] preventing the depletion of limited resources. The use of organic polymers for cathode-active materials has already achieved a high voltage and cycle performance comparable to those of traditional lithium-ion batteries.[7,9,10] 9,10-anthraquinone (AQ) and its derivatives are the most energy-rich anodic materials known, but their significant solubility in the electrolyte solutions influences their charge-discharge cycle number.[5] Compared to the pure component, the AQ functionalized carbon nanocomposites possess much higher active material utilization ratios and superior ultrafast-charge and discharge ability. For examples, the AQ-carbon fabric composite has been synthesized to obtain a high performance electrode material for supercapacitors,[11] and the AQ-graphene nanocomposite was developed as a highly efficient electrocatalyst for oxygen reduction reaction in alkaline conditions.[12] In all these applications, the interaction between the AQ (or its derivatives) and carbon materials especially graphene is required in order to obtain a

Journal of Materials Chemistry A Accepted Manuscript

comprehensive understanding of the superior electrochemical properties.

Two-dimensional graphene has rather unique electronic properties such as high migrate rate, massless carriers and anomalous quantum Hall effects.[13] The unique properties of the Dirac fermions suggest the potential of graphene to be a material for improving the performance organic electrodes of lithium-ion batteries. Recently, a structure analog of graphene, i.e., a sheet of heterogeneous boron nitride (BN), has been successfully isolated by Pacile et al.[14] and Han et al.[15] Although the hexagonal BN (*h*-BN) sheet has the same honeycomb lattice structure as graphene, its electronic properties are significantly different from those of graphene. Monolayer *h*-BN is a wide band gap semiconductor. The B-N bond in the layer has a character of dipole bonding interactions, underlying the charge transfer between B and N atoms. It is therefore interesting to carry out a theoretical research and compare the binding mechanism and the binding energy of the AQ and its derivatives on monolayer BN and graphene.

Among various theoretical approaches, *ab initio* density functional theory (DFT) has proved to be a powerful tool for the predictions of the binding energy.[16-19] Although DFT can easily deal with systems containing hundreds of atoms, the most widely used exchange-correlation DFTs, i.e., local density approximation (LDA), generalized gradient approximation (GGA) and standard hybrid DFT fail to treat the van der Waals (vdW) dispersion energy. However, a recent experimental and theoretical quantification of the adsorption enthalpies of organic molecules on graphene underlines the importance of non-local dispersion correlations.[20] The systems studied in this work contain aromatic interactions but are too large to be handled with standard wave functional theory. To accurately predict the inter- and intra-molecular noncovalent interactions, Grimme[21] proposed a general computational scheme for the parameters used in the damped

Journal of Materials Chemistry A Accepted Manuscript

atom-pairwise dispersion corrections of the form $C_6 \cdot R^{-6}$. The obtained parameters cover elements up to xenon and several common DFTs. The excellent results that have been obtained at affordable computational cost suggest the vdW dispersion-corrected DFT to be a routine tool for many applications in organic chemistry or biochemistry.[22-24] Random phase approximation[25] can also combat the shortcoming of the LDA, GGA and hybrid DFT, but it is computational expensive.

In this paper, a theoretical study on the adsorption of AQ and its derivatives, i.e., benzofuro[5,6-b]furan-4,8-dione (BFFD), benzo[1,2-b;4,5-b']dithiophene-4,8-dione (BDTD) and pyrido[3,4-g]isoquinoline-5,10-dione (PID), on the BN sheet and graphene was carried out. The vdW dispersion-corrected DFT was used to determine the binding energies for the adsorbed AQ and its derivatives. From the analysis of the calculated results, it is found that the vdW dispersion stabilization is dominant as it contributes more than 80% of the total attraction interaction for all the systems studied. Although the binding energy for a given molecule is very close on the BN sheet and graphene, the preferred adsorption site is definitely different due to the great difference in atomic polarizability between the BN sheet and graphene. A work function shift relative to an isolated BN sheet or graphene is found, indicating that an interfacial dipole between the adsorbate molecule and substrate has been induced by the strong physisorption.

2. COMPUTATIONAL DETAILS

The electronic structures and energies were obtained using the spin-polarized computations based on an *ab initio* DFT. The GGA in the Perdew-Burke-Ernzerhof parametrization (PBE)[26] implemented in DMol^3 package[27,28] was used to describe the electronic exchange and correlation effects. All core electrons were explicitly considered and some relativistic effects were introduced into the core. Version 4.4 of the double numerical plus polarization set was selected and confined

Journal of Materials Chemistry A Accepted Manuscript

within a global cutoff of 5.4 Å. The Brillouin zone sampling was applied to the 4×4×1 Monkhorst-pack *k*-point meshes. A 7×7 hexagonal graphene supercell with a length of 60 Å in the *z*-direction was used in all calculations. A thermal smearing with the value of 0.14 eV was applied to the orbital occupation to improve the self-consistent field convergence. All geometries were optimized until the maximum force acting on each atom and the maximum energy change were below 0.054 eV·nm^{-1} and 5.0×10^{-5} eV per atom, respectively. The electronic density of state (DOS) was computed for the most stable configurations on a 12×12×1 Monkhorst-pack *k*-point mesh. The geometric optimization process is the same as the previous work.[17]

Considering robustness and computational speed of the method for long-range electron correlations, the damped atom-pairwise dispersion corrections of the form $C_6 \cdot R^{-6}$ seem most promising. They prove high accuracy in many different applications.[22-24] A general form of the vdW force contribution is[21]

$$E_{\mathrm{vdW}} = -s_6 \sum_{i=1}^{N-1} \sum_{j=i+1}^{N} C_6^{ij} R_{ij}^{-6} f_{\mathrm{damp}}(R_{ij}, R_i^0, R_j^0) \quad (1)$$

where N is the number of atoms in the system, C_6^{ij} is the dispersion coefficient for atom pair ij, s_6 is a global scaling factor that only depends on the DFT used, R_{ij} is the distance between atoms i and j, R_i^0 is the vdW radii, and $f_{\mathrm{damp}}(R_{ij}, R_i^0, R_j^0)$ is a damping function to avoid near-singularities at small distances. In this work the C_6 coefficients and vdW radii determined by Grimme (DFT-D)[21] are used to evaluate binding energies.

The binding energy (E_{b}) was calculated from

$$E_{\mathrm{b}} = E_{\mathrm{sheet}} + E_{\mathrm{M}} - E_{\mathrm{M+sheet}} \quad (2)$$

where E_{sheet}, E_{M} and $E_{\mathrm{M+sheet}}$ are the energies of the pristine graphene or *h*-BN nanosheet, an isolated adsorbate molecule and an adsorbate molecule adsorbed on the nanosheet, respectively.

Journal of Materials Chemistry A Accepted Manuscript

The energy of an isolated adsorbate molecule was determined in a 60Å×60Å×60Å cell using a Mankhorst-Pack sampling of 5×5×5.

In addition to the binding energy, an absolute potential of the Fermi level, namely, the work function, is another important quantity in understanding field emission properties. The work function is defined as the energy needed to move an electron from the Fermi level to a vacuum. In this work, it is evaluated from

$$WF = \phi_0 e - E_F \quad (3)$$

where ϕ_0 is the electrostatic potential in a vacuum away from the surface, e is the electron charge and E_F is the Fermi energy.

2. RESULTS AND DISCUSSION

Before beginning adsorption calculations, we have optimized monolayer graphene and BN using the PBE, and PBE-D schemes. The calculated lattice constants and work functions for monolayer graphene and BN are listed in Table 1. For comparison, some previous theoretical[2] and experimental[29-33] results are also included in Table 1. The present work is in good agreement with the previous results. Thus the PBE-D scheme is selected in the adsorption calculations.

Adsorption of four battery active organic molecules on all high symmetry sites of graphene and the BN sheet are schematically investigated in this work, and they are drawn in Figure 1. The first kind of adsorption sites is labeled as "AA-stacking (AA)" in Figure 1(a), referring to that all carbon atoms in the middle C_6 ring of an adsorbate molecule sit on top of the atoms in a graphene or BN sheet. The second kind of adsorption sites shown in Figure 1(b) is "bridge-parallel (BP)", representing that one bond in a graphene or BN sheet is under the center and parallel to the two bonds in the middle C_6 ring of the organic molecule. The third and forth kinds of adsorption sites

Journal of Materials Chemistry A Accepted Manuscript

are labeled as "AB-stacking (AB)" and "bridge-slant (BS)" in Figure 1(c) and (d), respectively. The site labeled as "Cross" represents that all carbon atoms in the middle C_6 ring are located at top of the middle of C-C or B-N bond in a graphene or BN sheet. The last kind of adsorption sites is a shifted "Cross" (SC) configuration, which is obtained by shifting the organic molecule in the "Cross" configuration by half length of C-C or B-N bond.

The calculated binding energies E_b for the four organic molecules adsorbed on monolayer graphene using the PBE and PBE-D schemes are listed in Table 2. From Table 2 one can found that among six adsorption sites, the binding energy of the AQ and its derivatives on the BP site is the largest while the binding energy on the AA site is the smallest. The binding energies for the AQ and its derivatives on graphene are in the order: BDTD ≈ BFFD < AQ < PID using the PBE scheme and BFFD < BDTD < AQ < PID using the PBE-D scheme. The most stable adsorption configurations for the four organic molecules on monolayer graphene are illustrated in Figure 2. The equilibrium geometries of the four organic molecules on different sites of monolayer graphene can be found in Figures S1-4. Both the PBE and PBE-D schemes predict the same most stable configuration for the AQ and its derivatives on graphene. The preferred adsorption site shown in Figure 2 is different from that for benzene-graphene system obtained by Chang et al.[34] They have reported that the most stable configuration is the AB configuration for a benzene molecule adsorbed on monolayer graphene. This difference is not caused by the vdW interaction because of the lack of the dispersion correction in the PBE scheme. Perhaps it is due to that the strong electronic dipole between the polarized bonds (C=O) in the four organic molecules induces a charge distribution among the π electrons of carbon in graphene. It may also result from higher terms of the electrostatic interaction.

Journal of Materials Chemistry A Accepted Manuscript

The vertical distances between the organic molecules and a graphene layer can be found in Table 3. The calculated values of the vertical distance are in the range of 3.70-3.85 and 3.15-3.24 Å using the PBE and PBE-D schemes, respectively. It is found that the vertical distances are almost same on different sites for any systems using the same scheme, and they deviate from that on the preferred site by only ±0.01Å. The vertical distance calculated from the PBE-D shorter than that from the PBE scheme by 0.5-0.6 Å. From Tables 2 and 3 one can conclude that the PBE functional predicts lower binding energies and relatively larger vertical distances because the π-π stacking interactions between the organic molecules and graphene are not correctly described using it.

Figure 3 depicts the most stable configurations of the four organic molecules adsorbed on the BN nanosheet using the PBE-D scheme. From the figure one can see that the SC site is the preferred adsorption site for the AQ, BFFD and BDTD molecules, while the PID molecule is preferred to the AB site on the BN nanosheet. From Table 2 one can find that the most stable adsorption configuration for the AQ-BN system obtained using the PBE-D scheme is different from that using the PBE scheme, indicating that the vdW force in the SC site is stronger than that on the AB site for the AQ-BN system. The preferred adsorption configurations of the four organic molecules on the BN nanosheet are definitely different from those on the graphene nanosheet. This is mainly attributed to a more electrostatic attraction between the organic molecules and B atoms, and a less attraction between the organic molecules and N atoms due to the polar nature of the B-N bond. In addition, the vdW dispersion force has part of contribution on the preferred adsorption configurations, especially for the AQ-BN system. In Table 2, the binding energies of the four organic molecules on the BN nanosheet are in the order: BFFD < BDTD < PID <AQ

Journal of Materials Chemistry A Accepted Manuscript

using both the PBE and PBE-D schemes. As can be seen from Table 3, the values of the vertical distances between the organic molecules and the BN sheet predicted using the PBE and PBE-D schemes are in the range of 3.94-4.15 and 3.08-3.17Å, respectively. The values from the PBE-D scheme are shorter than the corresponding ones from the PBE functional for both adsorbate-graphene and adsorbate-BN systems. It is seen that the PBE functional predicts a slightly smaller binding energy on the BN nanosheet when compared with that on graphene. However, the PBE-D scheme predicts a very similar binding energy for each organic molecule adsorbed on monolayer graphene and BN, due to that the π-π stacking interactions on the BN nanosheet are very close to those on graphene.

In order to understand the influence of the vdW dispersion on the binding mechanics the total binding energy $E_{b,PBE-G}$ is decomposed as

$$E_{b,PBE-G} = E_{b,PBE} + E_{b,vdW} \quad (4)$$

where $E_{b,PBE}$ and $E_{b,PBE-G}$ are the binding energies calculated using the PBE and PBE-D schemes , respectively, and $E_{b,vdW}$ is the contribution of the vdW dispersion to the binding energy. Figures 4(a) and (b) depict the $E_{b,vdW}$ of the four organic molecules on monolayer graphene and BN, respectively. For all preferred adsorption sites on monolayer graphene and BN, the contribution of the vdW dispersion to the binding energy approximates to 1 eV. This indicates that the interactions between the four organic molecules and the graphene or BN nanosheet are the strong physisorption. As shown in Figure 4(a), the binding energies of the AQ, BFFD, BDTD and PID molecules on graphene predicted using the PBE-D scheme are larger than those using the PBE scheme by 1.047, 0.845, 0.904 and 1.040eV, respectively. The values of $E_{b,vdW}$ of the four organic molecules on the BP site of graphene are the largest and those on the AA site are the smallest

Journal of Materials Chemistry A Accepted Manuscript

among the six adsorption sites. Figure 4(b) shows that the value of $E_{b,vdW}$ on the SC site of the BN sheet is the largest for the AQ-BN, BFFD-BN, and BDTD-BN systems, while that on the AB site is the largest among the six sites for the PID-BN system. Similar to the systems of graphene, the contribution of the vdW dispersion is the smallest when the organic molecules are adsorbed on the AA site. The PBE-D scheme predicts $E_{b,vdW}$ = 1.108, 0.941, 0.974 and 1.089eV for the AQ-BN, BFFD-BN, BDTD-BN and PID-BN systems, respectively. Overall, the largest value of $E_{b,vdW}$ corresponds to the preferred adsorption site on monolayer graphene and BN. The magnitudes of $E_{b,vdW}$ for each organic molecule on the graphene and BN nanosheets are very close to each other, indicating that the value of $(C_6^{M\text{-}B} + C_6^{M\text{-}N})/2$ is quite near to the value of $C_6^{M\text{-}C}$, where M-B, M-N and M-C refer the atomic pairs between the constituent atoms in the organic molecule and the B, N and C atoms, respectively. If the dispersion contribution (in %) is calculated as $E_{b,vdW}/E_{b,PBE\text{-}G}$, it contributes more than 80% of the total attractive interact for all the complexes considered in this work.

The binding energies are related to the battery life when the organic compounds are used as an electrode. The strong binding energies between AQ (its derivatives) and graphene or BN can reduce the chemical potential of AQ (its derivatives). According thermodynamic principles, a compound with a lower chemical potential has a smaller solubility in a specific solvent. Therefore, introduction of graphene or BN to AQ (its derivatives) can prevent the unwanted dissolution in non-aqueous electrolyte of lithium-ion batteries that is suffered by AQ and its derivatives, and thereby increase the charge-discharge cycle number of the lithium-ion batteries. This makes the organic compound-graphene or organic compound-BN composite a promising electrode material of lithium-ion batteries. The above theoretical conclusion is expected to be validated by the related

Journal of Materials Chemistry A Accepted Manuscript

experimental data. Although there is no experimental data that can be used directly to validate this theoretical result, a recent experimental result reported by Song et al.[35] showed that the nanocomposites combining graphene with two promising polymer cathode materials, poly(anthraquinonyl sulfide) and polyimide, have surely achieved better cycling stability.

The total electronic density of state (DOS) and projected DOS (PDOS) for the four organic molecules adsorbed on the graphene and BN nanosheets are plotted in Figures 5 and 6, respectively. The basic shape of the DOS remains almost the same with respect to the pristine sheet. There is no evidence for hybridization between the four organic molecules and the intrinsic graphene or BN nanosheet. From analysis of the Mulliken charges using the PBE-D scheme, one can find a very small charge transfer between any of the four organic molecules and the graphene or BN nanosheet. The distribution of charge difference in real-space $\Delta\rho(\mathbf{r})$ can be obtained from

$$\Delta\rho(\mathbf{r}) = \rho_{\mathrm{M+sheet}}(\mathbf{r}) - \rho_{\mathrm{M}}(\mathbf{r}) - \rho_{\mathrm{sheet}}(\mathbf{r}) \quad (5)$$

where $\rho_{\mathrm{M+sheet}}(\mathbf{r})$, $\rho_{\mathrm{M}}(\mathbf{r})$ and $\rho_{\mathrm{sheet}}(\mathbf{r})$ are the charge density distributions in real-space of the molecule-substrate system, organic molecule and isolated graphene or BN nanosheet, respectively. Figures 7(a) and 7(b) depict $\Delta\rho(z)$ calculated from the PBE-D scheme for an AQ molecule adsorbed on the graphene and BN nanosheets, respectively. Because the electrostatic interactions are important for work function, the planar averaged electrostatic potentials calculated from the PBE-D scheme for the AQ-graphene and AQ-BN systems are plotted in Figures 8(a) and 8(b), respectively. An interfacial dipole can result from the charge rearrangement at the interface. This dipole causes a portion of work function shift. All work function shifts for the complexes studied in this work can be found in Table 3. As can be seen from the table, the work function shift is almost the same using the PBE and PBE-D schemes for each organic molecule on graphene. In

Journal of Materials Chemistry A Accepted Manuscript

contrast, for the BN monolayer, the work function shift from the PBE functional is smaller than that from the PBE-D scheme. The work function shifts obtained are in the order: AQ < BDTD <BFFD <PID for the organic molecules adsorbed on both graphene and BN nanosheets. The work function shift ΔWF can be understood from the expression given by

$$\Delta WF = \Delta\mu - ep/(A\varepsilon_0) \quad (6)$$

which is a modification of the work function expression proposed by Wigner and Bardeen,[36] and later by Lang and Kohm.[37] In Eq. (6), $\Delta\mu$ is the difference of the bulk chemical potential of electrons between the adsorption complexes and the pristine graphene or BN sheet, and the second term on right hand is the energy necessary to penetrate the dipole barrier at the surface, where p is the interfacial dipole, A is the area of the surface and ε_0 is the permittivity of free space. For the systems studied in this work, $\Delta\mu$ is strongly dependent on the ionization potentials of adsorbates. The work functions for the AQ, BFFD, BDTD and PID molecules obtained using the PBE-D scheme are 5.01, 5.28, 5.21 and 5.41 eV, respectively. These values dominate the sequence of the work function shift for the systems involved in this work. This conclusion is in coordinate with the results from the surface coverage work function model proposed by Longo et al.[38] Of course, surface dipole also has a contribution to the work function shift via the electrostatic relation included in Eq. (6).

The treatment of spin-unrestricted systems may be improved further since the results obtained from present PBE tend to favor delocalized solutions. The negative ionization potentials (IPs) and electron affinities of a test set of molecules were used by Zhang and Musgrave[39] to estimate the accuracies of 11 DFT functionals including the local spin density approximation (LDA), five GGAs, three hybrid GGA functional, one hybrid functional, and one hybrid meta GGA functional. They found that the highest occupied molecular orbital (HOMO) eigenvalues from the KMLYP,[40] BH&HLYP,[41] B3LYP,[42] PW91,[43] PBE[26] and BLYP[44] predict the negative IPs

Journal of Materials Chemistry A Accepted Manuscript

with average absolute errors of 0.73, 1.48, 3.10, 4.27, 4.33 and 4.41 eV, respectively. The GGAs predict the HOMO-lowest unoccupied molecular orbital (LUMO) gap relatively accurately with average absolute error of approximate 0.73 eV. Therefore, other DFT methods such as hybrids (KMLYP,[40] BH&HLYP,[41] or B3LYP[42]) may therefore improve the calculated binding energies as well as the binding energy orders.

3. CONCLUSIONS

The adsorption of the AQ, BDTD and PID molecules on monolayer BN and graphene has been investigated using both the PBE and PBE-D schemes. The binding energies obtained using the PBE-G scheme were larger than those using the PBE scheme. The contribution of the vdW dispersion to the binding energy ranges from 0.95 to 1.11 eV, which contributes more than 80% of the total attractive interaction for all the complexes studied in this work. In addition, they are close to each other for the four organic molecules on the BN and graphene nanosheets. The calculated binding energies are in the order: BFFD < BDTD < AQ <PID on the graphene nanosheet and BFFD < BDTD < PID < AQ on the BN nanosheet. The inclusion of the vdW dispersion correction results in a slightly larger work function shift and a shorter vertical distance between the organic molecules and the graphene or BN nanosheet when compared with those using the PBE functional. The strong physisorption induces an interfacial dipole between the organic molecules and the graphene or BN nanosheet, resulting in a portion of work function shift relative to the isolated graphene or BN nanosheet. The ionization potentials of the four organic molecules dominate the sequence of the work function shift as AQ < BDTD < BFFD < PID. The calculated results indicate that the AQ and its derivatives, i.e., BFFD, BDTD and PID, can be strongly bound to a graphene or BN nanosheet to reduce their solubility in the electrolyte solutions and enlarge the cycle number of batteries when they are used for electrode-active materials. Therefore, addition of the

Journal of Materials Chemistry A Accepted Manuscript

graphene or BN nanosheet to the materials composed of the AQ, BFFD, BDTD or PID molecule will improve their performance as environmentally friendly organic electrode materials of lithium-ion batteries.

ACKNOWLEDGMENTS

Here I would like to make an acknowledgement to Yong-Jun Du for her effort in collecting calculated data and preparing the manuscript. The author also greatly appreciates the financial supports of National Natural Science Foundation of China (No. 21376131).

REFERENCES

1 B. Scrosati and J. Garche, *J. Power Sources*, 2010, **195**, 2419-2430.

2 Y.-X. Yu, *J. Mater. Chem. A*, 2013, **1**, 13559-13566.

3 B. Dunn, H. Kamath and J. M. Tarascon, *Science*, 2011, **334**, 928-935.

4 J. Bhattacharya and C. Wolverton, *Phys. Chem. Chem. Phys.*, 2013, **15**, 6486-6498.

5 Y. Liang, Z. Tao and J. Chen, *Adv. Energy Mater.*, 2012, **2**, 742-769.

6 M. Armand and J.-M. Tarascon, *Nature*, 2008, **451**, 652-657.

7 Y. Morita, *Nature Mater.*, 2011, **10**, 947-951.

8 K. Karthikeyan, S. Amaresh, V. Aravindan, H. Kim, K. S. Kang and Y. S. Lee, *J. Mater. Chem. A*, 2013, **1**, 707-714.

9 H. Nishide and K. Oyaizu, *Science*, 2008, **319**, 737-738.

10 H. P. Wu, K. Wang, Y. N. Meng, K. Lu and Z. X. Wei, *J. Mater. Chem. A*, 2013, **1**, 6366-6372.

11 K. Kalinathan, D. P. DesRoches and X. Liu, *J. Power Sources*, 2008, **181**, 182-185.

12 G. Zhang, Y. Zhou, J. Chen and F. Yang, *Int. J. Electrochem. Soc.*, 2012, **7**, 11323-11337.

13 A. K. Geim, *Science*, 2009, **324**, 1530-1534.

14 D. Pacile, J. C. Meyer, C. O. Girit and A. Zettl, *Appl. Phys. Lett.*, 2008, **92**, 133107.

15 W.-Q. Han, L. Wu, Y. Zhu, K. Watanabe and T. Taniguchi, *Appl. Phys. Lett.*, 2008, **93**, 223103.

16 W. Kohn and L. J. Sham, *Phys. Rev.*, 1965, **140**, A1133-A1138.

Journal of Materials Chemistry A Accepted Manuscript

17 Y.-X. Yu, *Phys. Chem. Chem. Phys.*, 2013, **15**, 16819-16827.

18 Y. S. Meng and M. E. Arroyo-de Dompablo, *Energy Environ. Sci.*, 2009, **2**, 589-609.

19 A. M. Garay-Tapia, A. H. Romero and V. Barone, *J. Chem. Theory Comput.*, 2012, **8**, 1064-1071.

20 P. Lazar, F. Karlicky, P. Jurecka, M. Kocman, E. Otyepkova, K. Safarova and M. Otyepka, *J. Am. Chem. Soc.*, 2013, **135**, 6372-6377.

21 S. Grimme, *J. Comput. Chem.*, 2006, **27**, 1787-1799.

22 M. Piacenza and S. Grimme, *J. Am. Chem. Soc.*, 2005, **127**, 14841-14848.

23 M. Parac, M. Etinski, M. Peric and S. Grimme, *J. Chem. Theory Comput.*, 2005, **1**, 1110-1118.

24 J. Antony and S. Grimme, *Phys. Chem. Chem. Phys.*, 2006, **8**, 5287-5293.

25 X. G. Ren, P. Rinke, C. Joas and M. Scheffler, *J. Mater. Sci.*, 2012, **47**, 7447-7471.

26 J. P. Perdew, K. Burke and M. Ernzerhof, *Phys. Rev. Lett.*, 1996, **77**, 3865-3868.

27 B. Delley, *J. Phys. Chem.*, 1996, **100**, 6107-6110.

28 B. Delley, *J. Chem. Phys.*, 2000, **113**, 7756-7764.

29 B. T. Kelly. Irradiation damage in graphite due to fast neutrons in fission and fusion systems. In *Tech. Rep. TECDOC 1154 IAEA* Vienna, 2000.

30 D. D. L. Chung, *J. Mater. Sci.*, 2002, **37**, 1475-1489.

31 V. L. Solozhenko, G. Will and F. Elf, *Solid State Commun.*, 1995, **96**, 1-3.

32 Y.-J. Yu, Y. Zhao, S. Ryu, L. E. Brus, K. S. Kim and P. Kim, *Nano Lett.*, 2009, **9**, 3430-3434.

33 K. C. Kwon, K. S. Choi and S. Y. Kim, *Adv. Funct. Mater.*, 2012, **22**, 4724-4731.

34 C.-H. Chang, X. Fan, J.-J. Li and J.-L. Kuo, *J. Phys. Chem. C*, 2012, **116**, 13788-13794.

35 Z. P. Song, T. Xu, M. L. Gordin, Y.-B. Jiang, I.-T. Bae, Q. F. Xia, H. Zhan, J. Liu and D. H. Wang, *Nano Lett.*, 2012, **12**, 2205-2211.

36 E. Wigner and J. Bardeen, *Phys. Rev.* , 1935, **48**, 84-87.

37 N. D. Lang and W. Kohn, *Phys. Rev. B*, 1971, **3**, 1215-1223.

38 R. T. Longo, E. A. Adler and L. R. Falce, *1984 International Electron Devices Meeting*, 1984, **30**, 318-321.

39 G. Zhang and C. B. Musgrave, *J. Phys. Chem. A*, 2007, **111**, 1554-1561.

40 J. K. Kang and C. B. Musgrave, *J. Chem. Phys.*, 2001, **115**, 11040-11051.

Journal of Materials Chemistry A Accepted Manuscript

41 A. D. Becke, *J. Chem. Phys.*, 1993, **98**, 1372-1377.

42 A. D. Becke, *J. Chem. Phys.*, 1993, **98**, 5648-5652.

43 J. P. Perdew and Y. Wang, *Phys. Rev. B*, 1992, **45**, 13244-13249.

44 A. D. Becke, *J. Chem. Phys.*, 1988, **88**, 2547-2553.

Journal of Materials Chemistry A Accepted Manuscript

Table 1. Optimized lattice constant and work function of the graphene and BN nanosheets

	PBE	PBE-D	Expt
		Lattice constant (Å)	
Graphene	2.467	2.467	2.462[a]
BN	2.517	2.517	2.504[b]
		Work function (eV)	
Graphene	4.49(4.44[c])	4.49	4.57[d], 4.2[e]
BN	3.67	3.65	

[a] Experimental value from Kelly[29] and Chung.[30] [b] Experimental value from Solozhenko et al.[31] [c] Theoretical value taken from Yu.[2] [d] Experimental value from Yu et al.[32] [e] Experimental value from Kwon et al.[33]

Table 2. Calculated adsorption energy (in eV) for the AQ, BFFD, BDTD, and PID molecules on different adsorption sites of graphene and *h*-BN nanosheets

Adsorbate	DFT	AA	BP	AB	BS	Cross	SC
			Graphene				
AQ	PBE	0.243	**0.248**	0.244	0.243	0.247	0.243
	PBE-D	1.132	**1.295**	1.272	1.226	1.263	1.245
BFFD	PBE	0.197	**0.211**	0.209	0.205	0.201	0.202
	PBE-D	0.934	**1.056**	1.004	0.995	1.024	1.020
BDTD	PBE	0.204	**0.210**	0.210	0.216	0.215	0.210
	PBE-D	0.980	**1.114**	1.093	1.093	1.080	1.081
PID	PBE	0.249	**0.258**	0.256	0.250	0.254	0.250
	PBE-D	1.126	**1.298**	1.276	1.209	1.259	1.239
			h-BN				
AQ	PBE	0.196	0.196	**0.201**	0.198	0.197	0.189
	PBE-D	1.154	1.262	1.305	1.257	1.297	**1.309**
BFFD	PBE	0.152	0.148	0.157	0.150	0.155	**0.159**
	PBE-D	0.956	1.040	1.057	1.029	1.028	**1.100**
BDTD	PBE	0.163	0.156	0.168	0.161	0.165	**0.172**
	PBE-D	0.996	1.088	1.108	1.074	1.075	**1.146**
PID	PBE	0.193	0.182	**0.197**	0.190	0.183	0.187
	PBE-D	1.133	1.267	**1.286**	1.224	1.252	1.252

Journal of Materials Chemistry A Accepted Manuscript

Table 3. Calculated work function shift (in eV) and vertical distance (in Å) between an adsorbed molecule and a graphene or h-BN nanosheet at the preferred adsorption site.

Adsorbent	Adsorption sites	Work function shift (eV)		Vertical distance (Å)	
		PBE	PBE-D	PBE	PBE-D
		Graphene			
AQ	BP	0.03	0.05	3.79	3.19
BFFD	BP	0.11	0.11	3.70	3.16
BDTD	BP	0.08	0.11	3.85	3.24
PID	BP	0.19	0.19	3.72	3.15
		h-BN			
AQ	SC	1.22	1.31	4.15	3.13
BFFD	SC	1.39	1.47	3.94	3.08
BDTD	SC	1.36	1.41	4.12	3.17
PID	AB	1.52	1.55	4.11	3.08

Journal of Materials Chemistry A Accepted Manuscript

Figure captions

Figure 1. Adsorption sites of an AQ molecule on a graphene or BN monolayer.

Figure 2. Optimized structures of (a) AQ, (b) BFFD, (c) BDTD and (d) PID molecules on a graphene monolayer.

Figure 3. Optimized structures of (a) AQ, (b) BFFD, (c) BDTD and (d) PID molecules on a BN monolayer.

Figure 4. Calculated vdW contributions $E_{b,vdW}$ for AQ, BFFD, BDTD and PID molecules adsorbed on graphene and h-BN monolayers.

Figure 5. Total and projected DOS for the most stable adsorption configurations from the PBE-D scheme: (a) DOS for the AQ-graphene and BFFD-graphene systems, (b) PDOS for the AQ-graphene system, (c) PDOS for the BFFD-graphene system, (d) DOS for the BDTD-graphene and PID-graphene systems, (e) PDOS for the BDTD-graphene system and (f) PDOS for the PID-graphene system. The arrows denote spin-up (↑) and spin-down (↓) states.

Figure 6. Total and projected DOS for the most stable adsorption configurations from the PBE-D scheme: (a) DOS for the AQ-BN and BFFD-BN system, (b) PDOS for AQ-BN system, (c) PDOS for BFFD-BN system, (d) DOS for the BDTD-BN and PID-BN systems, (e) PDOS for the BDTD-BN system and (f) PDOS for the PID-BN system. The arrows have the same meaning as in Figure 5.

Figure 7. The charge difference profiles between the adsorption system and the isolated systems along the *z*-direction for (a) the AQ-graphene and (b) the AQ-BN systems. The vertical dashed lines represent the position of the monolayer (z = 0) and AQ molecule.

Journal of Materials Chemistry A Accepted Manuscript

Figure 8. The planar averaged electrostatic potentials along he *z*-direction for (a) the AQ-graphene and (b) the AQ-BN systems. The vertical dashed lines have the same meaning as in Figure 7.

Journal of Materials Chemistry A Accepted Manuscript

Figures of
Manuscript ID TA-ART-01-2014-000103-R1

Journal of Materials Chemistry A Accepted Manuscript

Fig. 1

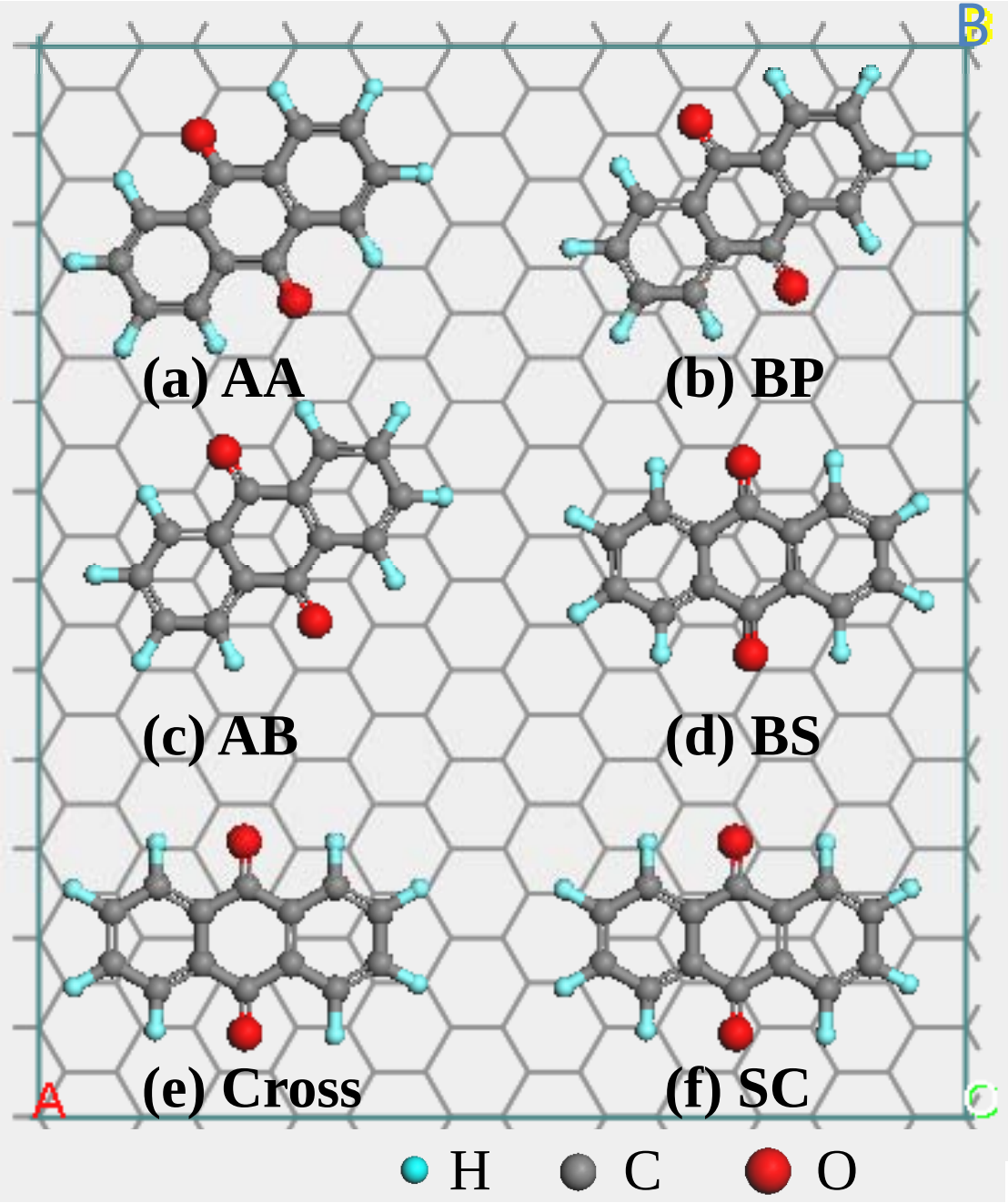

Journal of Materials Chemistry A Accepted Manuscript

Fig. 2

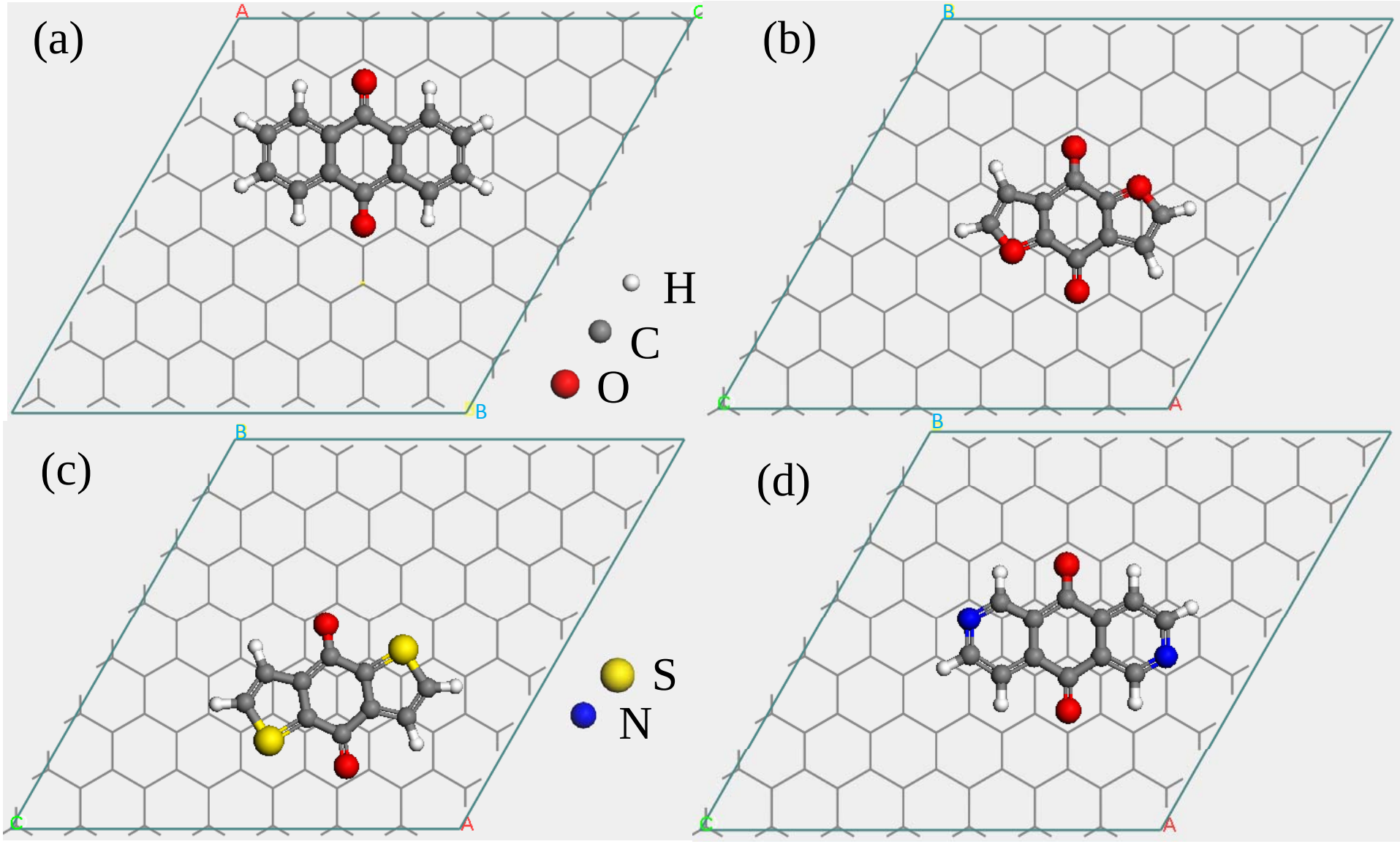

Journal of Materials Chemistry A Accepted Manuscript

Fig. 3

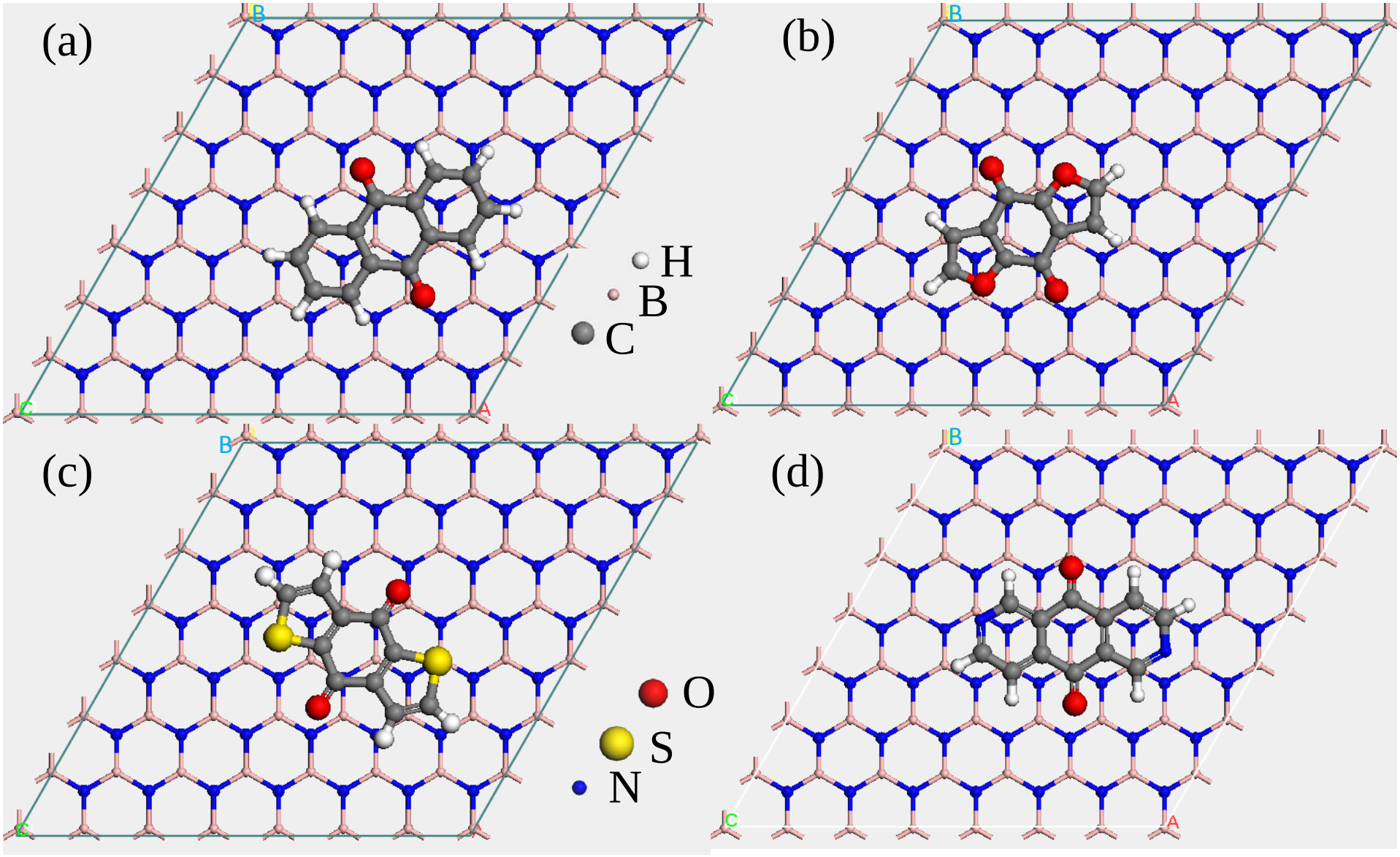

Journal of Materials Chemistry A Accepted Manuscript

Fig. 4

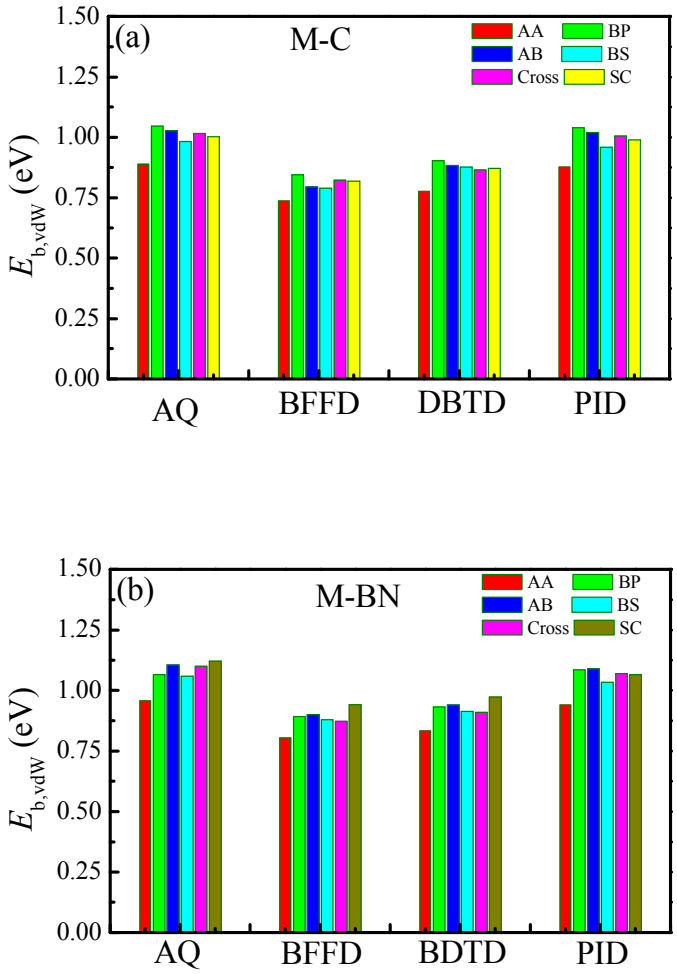

Journal of Materials Chemistry A Accepted Manuscript

Fig. 5

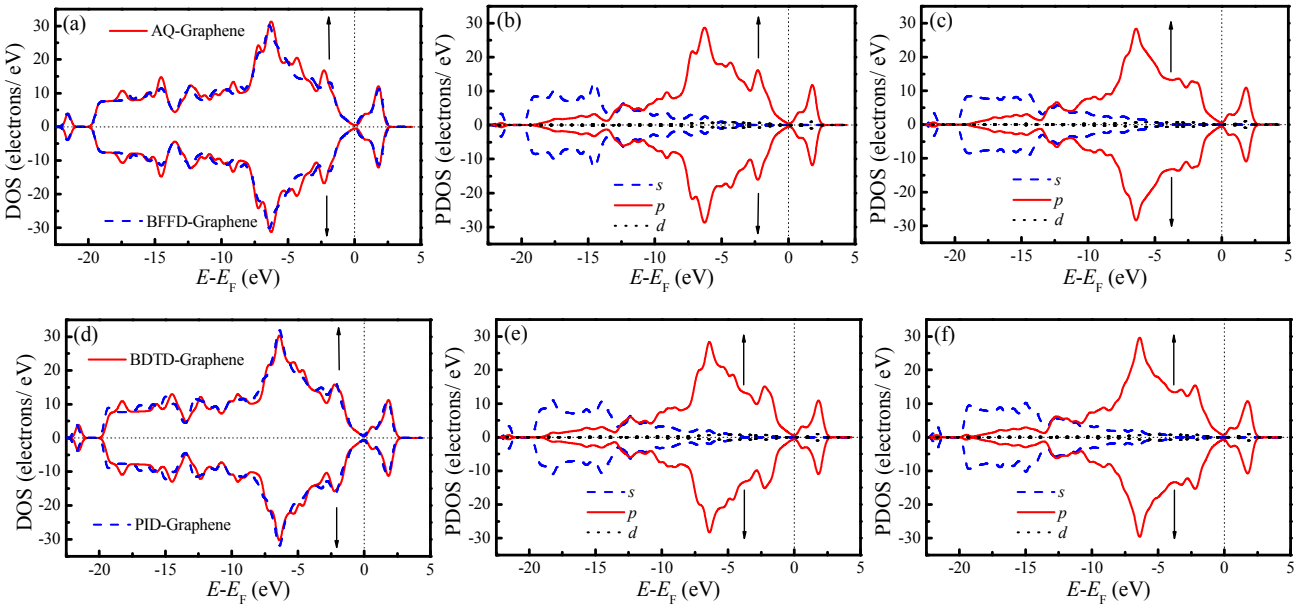

Journal of Materials Chemistry A Accepted Manuscript

Fig. 6

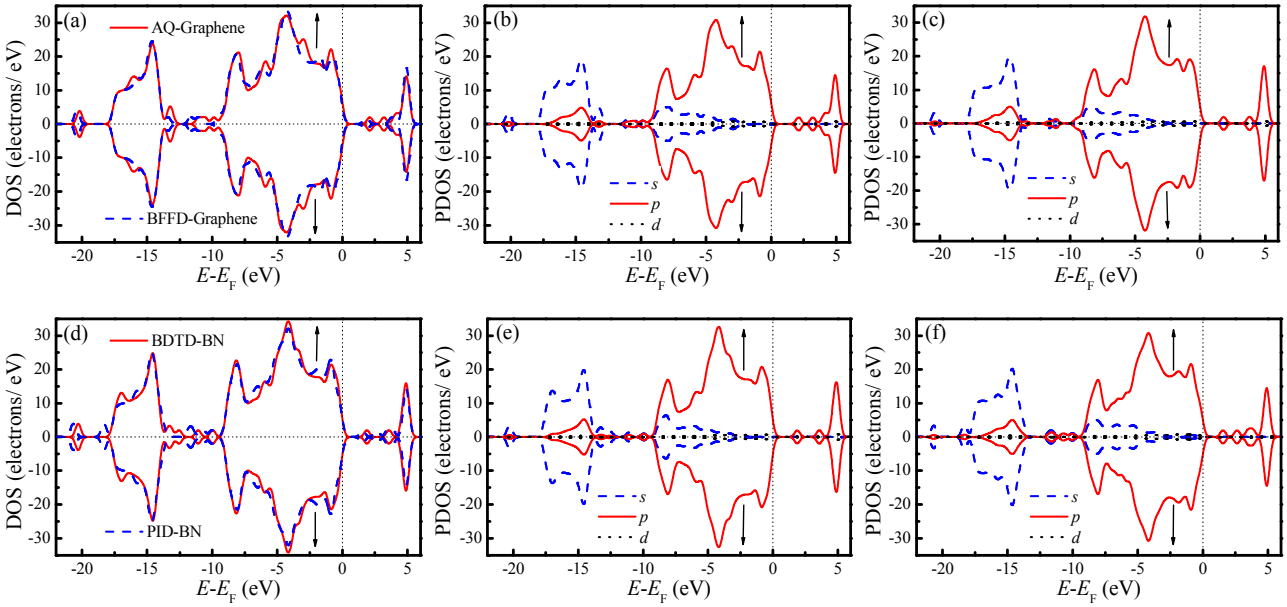

Journal of Materials Chemistry A Accepted Manuscript

Fig. 7

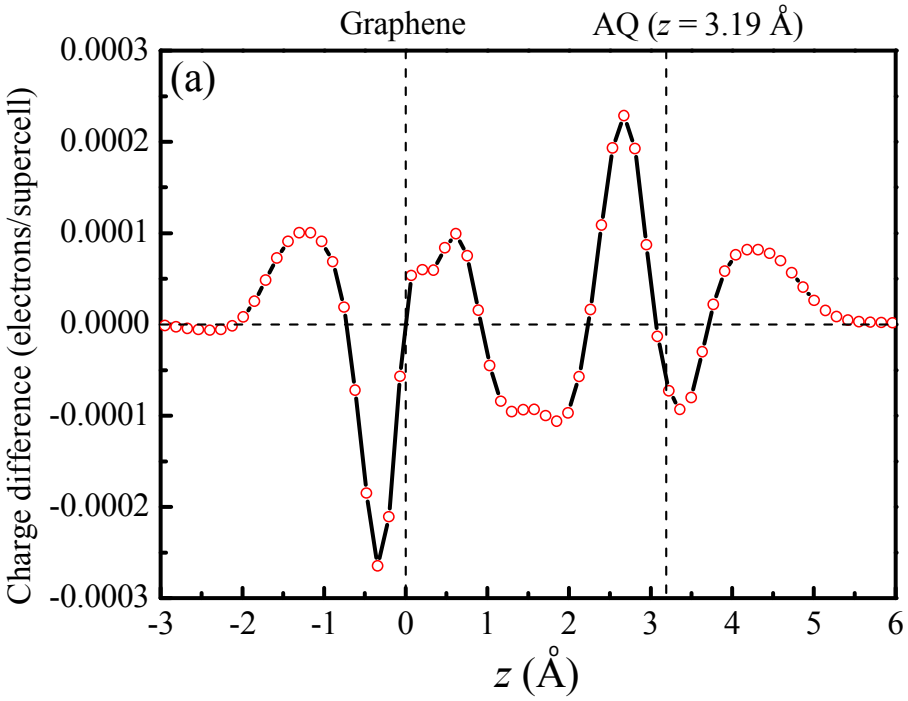

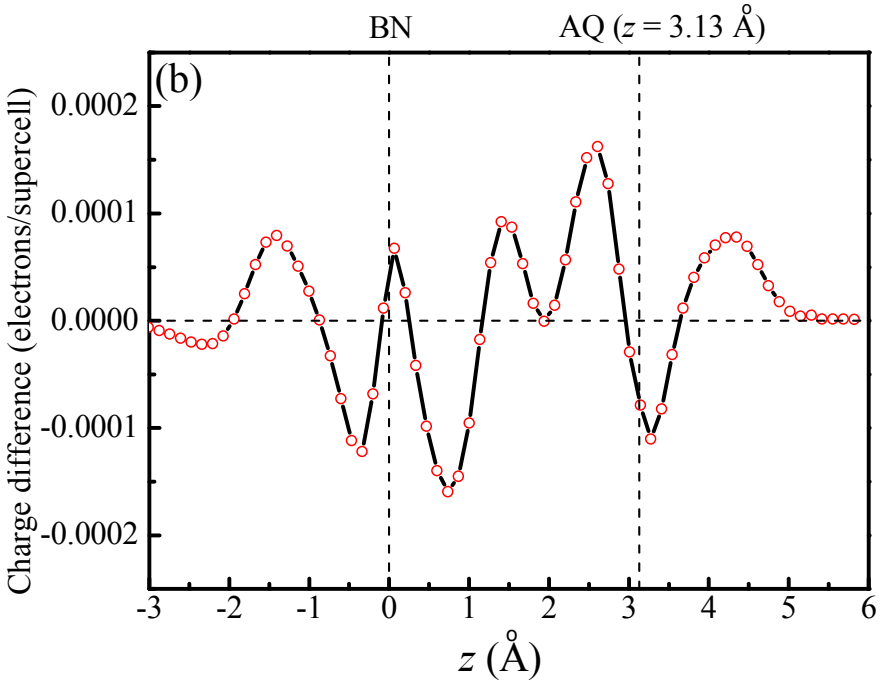

Journal of Materials Chemistry A Accepted Manuscript

Fig. 8

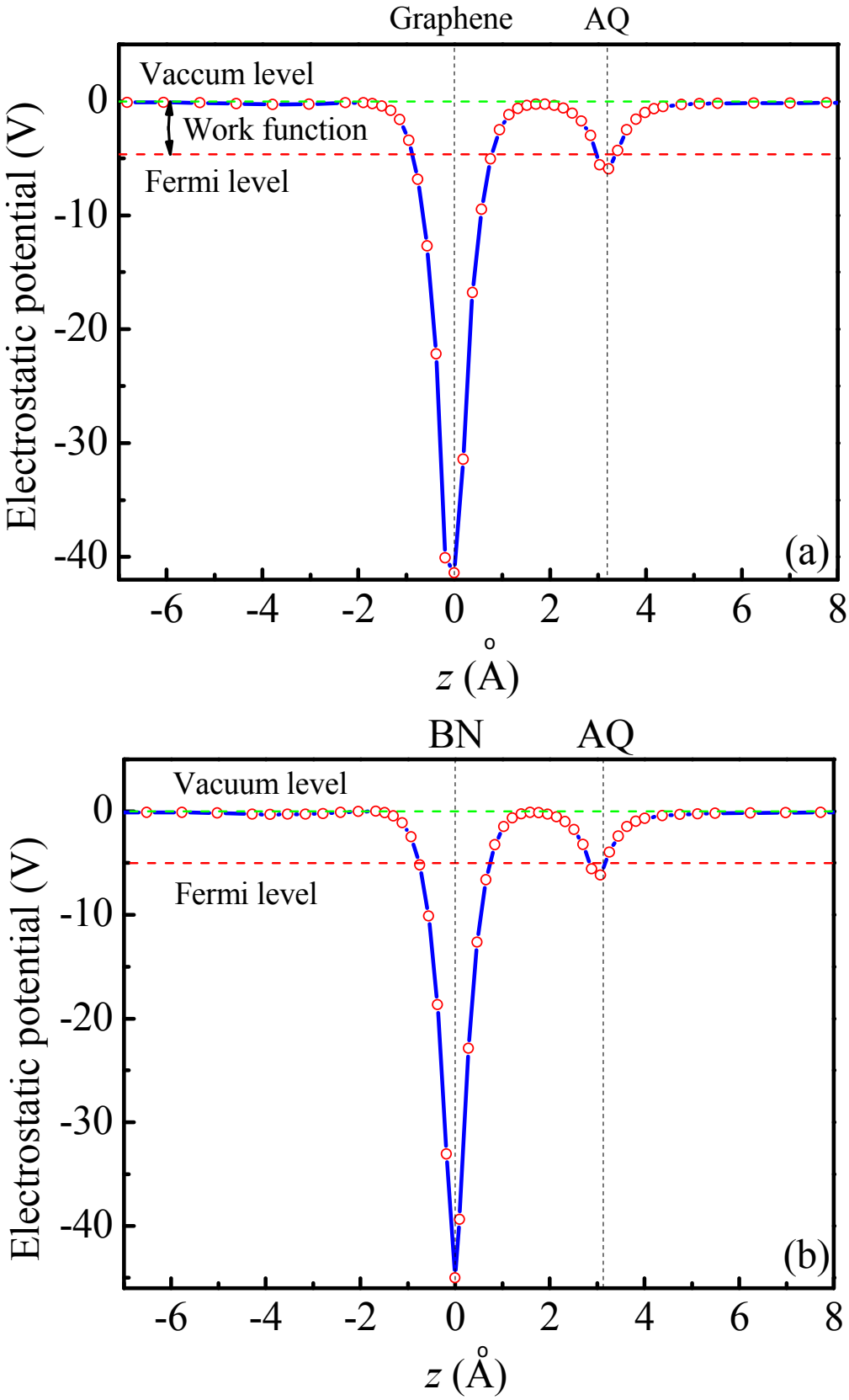

Journal of Materials Chemistry A Accepted Manuscript